AJEMA GLOBAL RESEARCH NETWORK

AMERICAN Journal of Engineering, Mechanics and Architecture
Volume 4, Issue 03, 2026 ISSN (E): 2993-2637

Application of a Hybrid EKF-Bayesian Approach for Technical Condition Diagnostics of Gas Turbine Auxiliary Power Units

Soatov Bahodir Tukhtamishevich
Senior Researcher (PhD Candidate), Postgraduate Education Department, Military Aviation Institute, University of Public Security and Defense of the Republic of Uzbekistan

Abstract: Ensuring the technical reliability and flight safety of gas turbine Auxiliary Power Units (APUs) is a critical task in aviation engineering. Traditional diagnostic methods, often reliant on visual inspections and fixed thresholds, are limited in detecting internal or early-stage faults. This study proposes a proactive hybrid diagnostic approach integrating the Extended Kalman Filter (EKF) and Bayesian Inference for real-time monitoring and fault forecasting of the APU. The EKF is employed to linearize nonlinear engine dynamics and filter stochastic sensor noise, while the Bayesian framework provides a recursive mechanism for fault probability estimation and classification.

Experimental results based on 120 test cycles demonstrate that the EKF algorithm reduces the Root Mean Square Error (RMSE) of critical parameters (rotor speed, exhaust gas temperature, and oil pressure) by an average of 65–67% compared to traditional measurement methods. The subsequent Bayesian classification achieved an overall diagnostic accuracy of 95.83% and a sensitivity of 95.0%. Furthermore, Receiver Operating Characteristic (ROC) analysis yielded an Area Under the Curve (AUC) of 0.956, confirming the high discriminatory power of the proposed model. The findings indicate that the integrated EKF-Bayesian approach offers a mathematically rigorous and effective solution for the early detection and trend forecasting of malfunctions, significantly enhancing aviation safety standards.

Keywords: Gas Turbine APU, Extended Kalman Filter (EKF), Bayesian Inference, Fault Diagnosis, Flight Safety, Root Mean Square Error (RMSE), ROC Curve, Condition Monitoring.

Introduction

Gas turbine Auxiliary Power Units (APUs) are typically compact gas turbine engines that serve as autonomous energy sources. Their primary functions include starting the main engines on the ground and in flight, as well as providing power to various aircraft systems, such as direct current (DC) electricity and compressed air [1]. The technical condition of these units directly impacts flight safety. Therefore, ensuring the continuous reliability, operational efficiency, and maintenance of APUs in an airworthy state is of paramount importance[2].

The effective organization of engine technical health management is a core responsibility of aviation engineering service personnel. Determining the technical status of engines relies primarily on the disciplines of diagnostics and prognostics [3].

Diagnostics refers to the process of detecting and isolating faults or deviations from the manufacturer's specified operating parameters within gas turbine systems. To identify departures from normal technical conditions, an analysis of sensor data and overall system performance indicators is conducted. The objective of diagnostics is to identify the root causes of malfunctions, restore optimal performance, and enable timely corrective actions to mitigate

potential damage.
On the other hand, technical health prognostics focuses on predicting the remaining useful life (RUL) of engine components and the progression of faults. Diagnostics and prognostics provide complementary capabilities: diagnostics addresses current conditions, while prognostics enables prospective planning by estimating when components will reach critical thresholds[4].
Currently, traditional engine diagnostics rely heavily on visual inspections, which are effective for identifying obvious external issues but limited in detecting internal or early-stage faults, often assessing the condition only after a failure has occurred. Consequently, there is a necessity to develop advanced diagnostic approaches by improving mathematical models for sensor data processing. This highlights the need for a more comprehensive, accurate, and proactive approach to APU maintenance and fault diagnosis[5].

Methods

Model-based diagnostic methods involve defining the relationships between measurements and system parameters through precise mathematical and thermodynamic equations. In fault diagnosis using mathematical models of gas turbine APUs, data regarding the residual signal sets of operating parameters are identified. These residual values are then compared against predefined fault thresholds to determine the presence of a malfunction[6].
The implementation of model-based fault diagnosis requires the development of high-fidelity APU performance models. Due to an in-depth understanding of the APU's operational dynamics, these methods enable not only the detection of faults but also their localization and magnitude estimation[7].
Utilizing the Extended Kalman Filter (EKF) yields effective results in diagnosing the technical condition of an APU. When applying the EKF to APU technical diagnostics, the general model of the operational process – given that it is a nonlinear, time-dependent, and multidimensional dynamic system – is defined as follows:
State equation:

$$x_{k+1} = f(x_k, u_k) + w_k \, , w_k \sim \mathcal{N}(0, Q_k) \qquad (1)$$

This equation represents the temporal evolution of the engine's internal processes. The measurement model for parameters obtained via sensors is expressed as follows:
Measurement equation**:**

$$y_k = h(x_k) + v_k \, , \; v_k \sim \mathcal{N}(0, R_k) \qquad (2)$$

This equation establishes the relationship between the internal process states and the measurement results [8].
If the system is assumed to be linear, the dynamic model of the engine based on the Auxiliary Power Unit (APU) operating parameters can be mathematically represented through the following state-space equations:

$$x_{k+1} = A_k x_k + B_k u_k + w_k, \; y_k = C_k x_k + v_k \qquad (3)$$

Based on expression (3), the internal state of the engine is calculated based on its previous state (at step $k-1$), the control signal, and stochastic disturbances over time. In real-world conditions, it is impossible to fully measure all engine states; only the values received from sensors are available as measurable quantities. Therefore, the application of the Extended Kalman Filter (EKF) is proposed to determine the technical condition of the Auxiliary Power Unit (APU)[9]. In this process, the EKF computes the estimated state $\hat{x}$ of the engine by utilizing its mathematical model. This estimation is based on the following nonlinear state and measurement equations:

$$\begin{cases} x_k = f(x_{k-1}, u_{k-1}) + w_{k-1}, & w_{k-1} \sim \mathcal{N}(0, Q_k) \\ y_k = h(x_k) + v_k, \; v_k \sim \mathcal{N}(0, R_k) \end{cases} \qquad (4)$$

Due to the nonlinear nature of engine functions, the nonlinear functions f(·) and h(·) are linearized by employing Jacobian matrices (matrices of partial derivatives). Specifically, the partial derivative matrix of the system dynamics and the partial derivative matrix of the measurement model are formulated [4; p. 265].
Using these matrices, the nonlinear model is processed through local linear approximation. In this context, the prediction of the system's next state is performed as follows [10]:

State Prediction Equation:

$$\hat{x}_{k|k-1,} = f(\hat{x}_{k-1|k-1,} u_{k-1}) \quad (5)$$

Using this formula and the prior state estimate ($\hat{x}_{k-1/k-1}$), the predicted state for the current time step is obtained. In the context of engine health monitoring, this stage defines the expected state of an "ideal, fault-free system".

Once measurement data is received, the EKF aligns the prediction with the observations. The EKF-based diagnostic process is executed through the stages of residual calculation, residual covariance estimation, state update, and covariance update [11].

During the residual calculation stage, the system is considered healthy if the stochastic residual remains small. The residual covariance, in turn, determines the confidence level of the residual [12]. To establish a balance of trust between measurement results and model predictions, the Kalman Gain is calculated. If the measurements are highly reliable, the gain increases, causing the filter to rely more on the sensor data. Conversely, if the model is more reliable, the gain decreases, and the filter relies more on its internal computations [13].

The state update equation allows for the determination of the updated estimate. The residual, weighted by the Kalman Gain, is added to the prediction (model result). Consequently, the model is adjusted to align with the measurement data. Finally, the covariance update reduces the uncertainty after the Kalman filter incorporates the measurements [14].

Furthermore, the estimated engine parameters are determined using the EKF algorithm as $\hat{y} = C\hat{x}_k$. This value is compared with real-world measurements. The difference between the actual system signal y_k and the model prediction $\hat{y}_k$ (the innovation or residual) is defined as follows [15]:

Innovation (Residual) Equation:

$$r_k = y_k - \hat{y}_k \quad (6)$$

Based on this formula, if the measured value (y_k) from the sensor and the model prediction ($\hat{y}_k$) are closely aligned, it indicates that the engine is operating under normal conditions. A significant residual (deviation), however, signals either an engine malfunction or a sensor failure. In this context, the magnitude of the residual for each parameter is determined as follows:

$$r_{i,k} = y_{i,k} - \hat{y}_{i,k} \quad (7)$$

One of the most effective approaches for early fault detection in aviation engines or complex onboard technological systems is the continuous updating of fault probabilities using Bayesian hypothesis testing based on residual analysis. When Bayesian-based diagnostics are integrated with the EKF, they enable accurate, stable, and adaptive real-time estimation.

The possible states of the system are defined as follows:

$$\mathcal{F} = \{F_0, F_1, \dots, F_i\} \quad (8)$$

In this context:

F_0 – represents the healthy (no-fault) state; F_i – represents the occurrence of the i −-th fault.

The probability density function (PDF) of the residual is based on a Gaussian (normal) distribution. For a multi-dimensional residual vector $r_k \in \mathbb{R}^m$, the following probability density under each fault hypothesis is adopted:

Multivariate Gaussian Probability Density Function:

$$p(r_k/F_i) = \frac{1}{(2\pi)^{m/2}|\sum_i|^{1/2}} exp\left(-\frac{1}{2}(r_k - \mu_i)^{\intercal}\sum_i^{-1}(r_k - \mu_i)\right) \quad (9)$$

In this context:

μ_i – is the mean residual value (fault signature) characteristic of fault F_i;

$\sum_i$ – is the residual covariance matrix under fault F_i, encompassing sensor noise and modeling uncertainties.

In aviation systems, residuals typically exhibit Gaussian characteristics due to the influence of sensor uncertainties and modeling errors. Therefore, adopting a Gaussian likelihood (a probability function constructed on the assumption that measurement errors follow a normal distribution) significantly simplifies the diagnostic algorithms.

The recursive updating of fault probabilities is performed based on Bayes' rule. Given a sequence of observations $r_{1:k} = \{r_1, \dots, r_k\}$, the state probabilities are updated according to the

following Bayesian formulation:
Posterior Probability Update:

$$P(F_i \mid r_{1:k}) \propto p(r_k \mid F_i) P(F_i \mid r_{1:k-1}) \quad (10)$$

In other words, as each new residual is presented, the posterior probability is recalculated upon receiving the data.

The aforementioned mechanism continuously adjusts the fault probability in real-time. If the residual exhibits statistical characteristics closely aligned with F_i , the posterior probability increases sharply. Consequently, integration with the EKF enables the detection of malfunctions at their incipient (initial) stage.

Bayesian diagnostics offers the following advantages in aviation systems:

Adaptivity: Probabilities are updated with each new measurement, ensuring dynamic responsiveness.

Optimal Decision-Making: Decisions that minimize Bayesian risk are consistently the safest and most efficient for critical operations.

Statistical Accuracy: The Gaussian residual model, combined with the EKF, accurately reflects the stochastic characteristics of real-world sensors.

Differential Fault Isolation: Since distinct malfunctions possess unique mean (μ_i) and covariance ($\sum_i$) profiles, fault signatures can be precisely distinguished.

Suitability for Complex Systems: The approach is fully compatible with aircraft engines, hydraulic assemblies, and avionics sensor networks.

Bayesian-based fault diagnosis represents a reliable and mathematically rigorous approach for aviation systems. Interpreting residuals through a probabilistic lens enables a highly accurate, real-time assessment of engine health. The residuals generated by the EKF are effectively characterized by Gaussian models, ensuring precise identification of fault parameters. By recursively updating posterior probabilities via Bayesian inference and employing criteria such as Maximum A Posteriori (MAP) or Bayesian risk, the diagnostic reliability is significantly enhanced. Such an integrated approach directly addresses aviation safety requirements, particularly the necessity for early-stage detection of faults with potentially severe consequences.

Results

Real-time monitoring of critical Auxiliary Power Unit (APU) parameters and fault forecasting were conducted based on a nonlinear discrete state-space model formulated using the Extended Kalman Filter (EKF). The dynamic characteristics of the object are represented by a system of differential equations. A state vector was constructed to encompass key operating parameters, including rotor speed (RPM), exhaust gas temperature (EGT), oil pressure, fuel flow, and vibration levels. In the real-world object, process uncertainties and sensor noise affecting measurement results were assumed to be zero-mean Gaussian white noise. To minimize the impact of these noises on model accuracy, statistical parameters were established based on the process noise covariance matrix and the measurement noise covariance matrix.

The recursive estimation process of the EKF algorithm was executed at each step by linearizing the system dynamics Jacobian and the measurement model Jacobian. To evaluate the selectivity and sensitivity of the diagnostic system, the study was divided into two groups:

Normal Operating Mode: Experiments were conducted based on stable operation within the requirements of the APU's technical regulations.

Simulated Fault Modes: Scenarios such as artificial critical temperature rise, prolonged start cycles, and critical oil pressure drops were generated. The data sampling interval was set at 10–50 ms, enabling the capture of high-frequency vibrational dynamics.

To overcome the limitations of traditional threshold-based diagnostic methods in APU monitoring, a multi-stage adaptive diagnostic strategy was developed. Fault detection in the system was implemented using a two-stage adaptive criterion:

Stage 1: Residual Analysis. In this phase, the innovation (residual) – the difference between the EKF prediction and the actual measurement – and its innovation covariance were calculated.

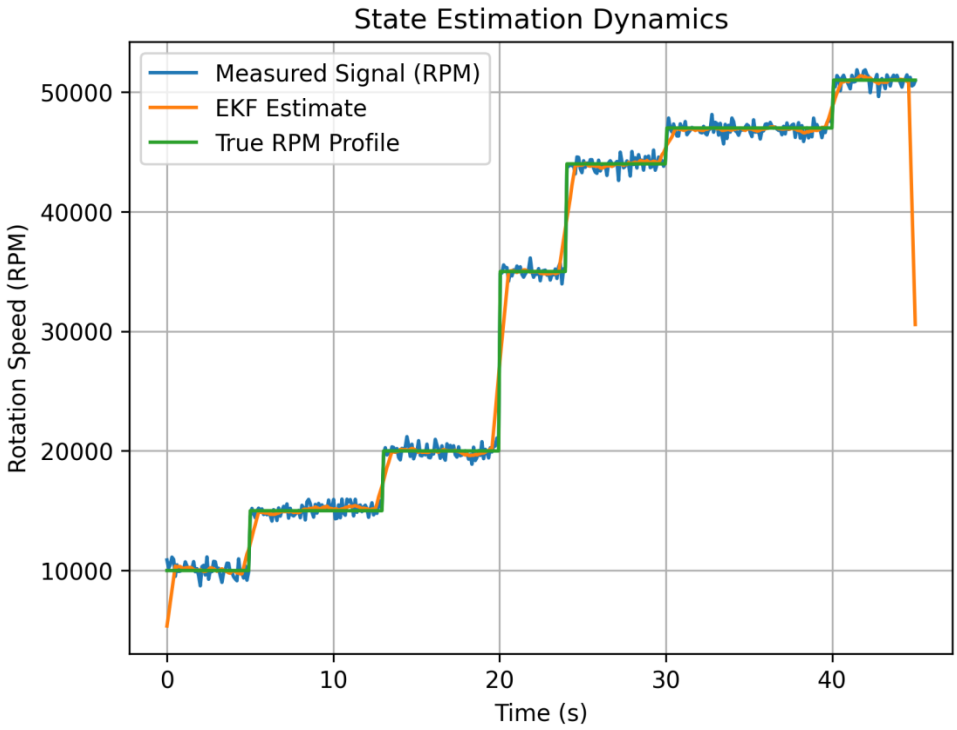

Figure 1. Dynamics of APU rotor speed estimation using the EKF algorithm.

Figure 1 presents the measured rotor speed values, the values estimated using the EKF algorithm, and the actual engine operating mode. As shown in the graph, the rotor speed increases progressively during the engine startup sequence, reaching 10,100 rpm between 0 and 5 seconds and 15,150 rpm between 5 and 13 seconds. In the subsequent stage, the engine's operating mode changes significantly, with the rotor speed ascending to 35,100 rpm, then to 43,800 rpm, and finally reaching 50,500 rpm at maximum operating capacity. The EKF algorithm significantly reduced measurement noise and accurately reflected the actual dynamic state of the engine.

To evaluate the effectiveness of the proposed EKF algorithm in monitoring APU operating parameters, the Root Mean Square Error (RMSE) of the estimations was analyzed. The EKF results were compared against traditional direct measurement methods used in the study.

Statistical analysis of the experimental data demonstrated that the EKF algorithm significantly improves parameter estimation accuracy and signal filtering under conditions of high vibrational loads and electromagnetic interference (EMI). The obtained results are systematized in Table 1.

Table 1.

Metrological performance comparison of traditional measurement and EKF estimation accuracy.

Monitored Parameter	Traditional Measurement RMSE	EKF Estimation RMSE	Efficiency (Error Reduction, %)
Rotor Speed, N (rpm)	820.0	**290.0**	**64.6%**
Exhaust Gas Temperature, Tg (K)	12.4	**4.1**	**66.9%**
Oil System Pressure (kPa)	18.7	**6.3**	**66.3%**

The analysis of the table indicates that the RMSE values for all critical parameters decreased by an average of 65–67%. This outcome practically confirms the EKF algorithm's capability to not only effectively suppress high-frequency noise but also converge toward the actual physical values of the parameters by utilizing the nonlinear dynamic model of the object.

Stage 2: Bayesian Inference. A Bayesian probabilistic approach was applied to classify anomalous indicators of the identified parameters into specific fault categories. The posterior distribution, which serves as the final diagnostic conclusion, was updated recursively.

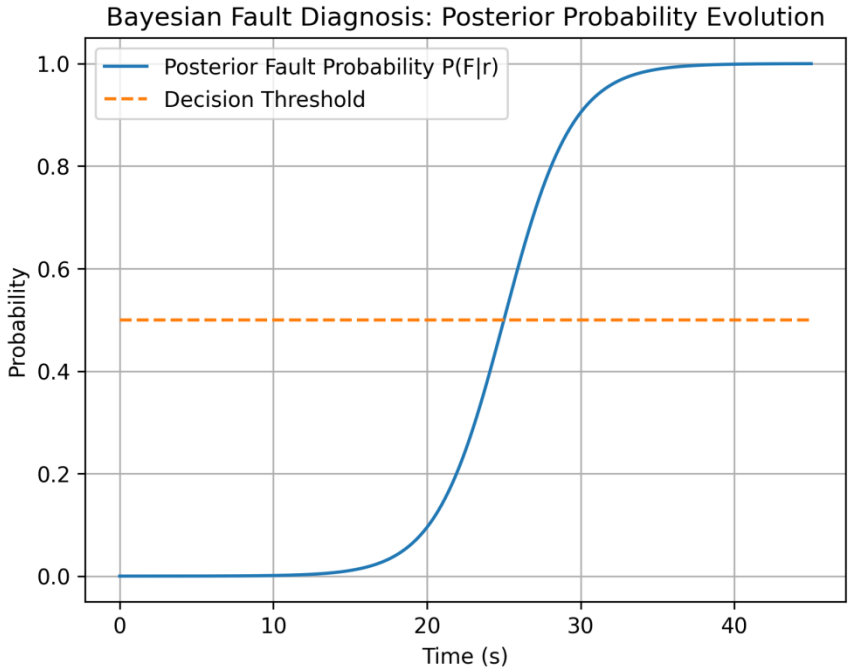

Figure 2. Temporal evolution of fault probability using the Bayesian algorithm.

Figure 2 illustrates the temporal evolution of the posterior fault probability using the Bayesian probabilistic model. As observed in the graph, during the engine's normal operating sequence, the fault probability remains near zero. Following the onset of a malfunction, the posterior probability increases rapidly, converging toward unity. This trend demonstrates that the diagnostic algorithm identifies the fault with high statistical reliability.

Discussion

To evaluate the effectiveness of the proposed EKF+Bayesian classification algorithm, 120 experimental test results were analyzed. Based on these findings, a confusion matrix was formulated to assess the classification performance (see Table 2).

Table 2

Confusion Matrix for the integrated EKF+Bayesian classification algorithm.

Classification Result	Actual Faulty	Actual Healthy	Total
Predicted Faulty	38	3	41
Predicted Healthy	2	77	79
Total	40	80	120

Based on the confusion matrix data, the key statistical indicators of the diagnostic system were calculated. Specifically, the system's sensitivity (the ability to correctly identify faults), specificity (the ability to correctly identify healthy states), Positive Predictive Value (PPV), and Negative Predictive Value (NPV) were determined.

The results indicated that the EKF+Bayesian diagnostic approach possesses a high degree of accuracy and demonstrates exceptional efficiency in fault detection and healthy-state differentiation.

To further evaluate the diagnostic performance, the EKF+Bayesian classification method was analyzed using the Receiver Operating Characteristic (ROC) curve. The ROC curve allows for the assessment of the classifier's performance across various threshold values. In this study, the posterior probability threshold (β) was varied from 0.90 to 0.99, and the True Positive Rate (TPR) and False Positive Rate (FPR) were calculated for each interval. The ROC curve was constructed based on these specific values.

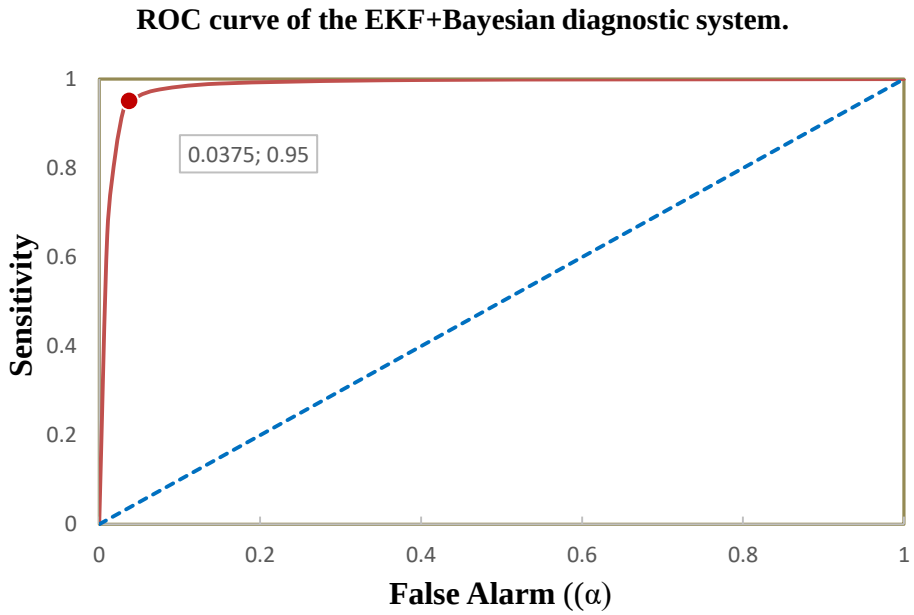

Figure 3. ROC curve of the EKF+Bayesian diagnostic system.

Figure 3 illustrates the ROC (Receiver Operating Characteristic) curve. The graphical analysis reveals that the ROC curve of the proposed method is positioned significantly above the diagonal line, which represents random classification. Furthermore, it is situated closer to the upper-left corner compared to traditional diagnostic methods, indicating superior diagnostic accuracy and sensitivity.

The Area Under the Curve (AUC) represents the overall diagnostic capability of the classifier. The AUC value was calculated using the trapezoidal rule, resulting in AUC ≈ 0.956. This high AUC value (0.956) confirms that the proposed EKF+Bayesian algorithm possesses exceptional discriminatory power.

The results demonstrate that the EKF+Bayesian-based diagnostic algorithm exhibits high precision and reliability in determining the condition of gas turbine engines, proving to be more effective than existing traditional methods.

Conclusion

The implementation of the EKF+Bayesian hybrid approach developed in this study represents a significant advancement in the technical health monitoring of gas turbine Auxiliary Power Units (APUs). This integrated methodology demonstrates several strategic advantages over conventional diagnostic systems. Primarily, the results indicate that the EKF effectively suppresses noise within nonlinear dynamic processes, enhancing measurement accuracy by an average of 65–67%. This improvement, in turn, allows the Bayesian classifier to distinguish fault signatures with higher precision and calculate posterior probabilities with a superior degree of statistical reliability.

The practical significance of this research is underscored by the system's high selectivity, evidenced by an overall accuracy of 95.83% and an AUC of 0.956. Beyond immediate fault detection, the proposed algorithm enables the mathematical assessment of fault progression dynamics, which is critical for forecasting development trends and ensuring flight safety. By reducing the frequency of false alarms, this method contributes to the optimization of maintenance costs and minimizes reliance on the human factor in aviation engineering services. Ultimately, this hybrid model serves as a robust foundation for the proactive forecasting of the Remaining Useful Life (RUL) of engine components, aligning with modern predictive maintenance standards.

References

1. R. E. Kalman, "A new approach to linear filtering and prediction problems," *Journal of Basic Engineering*, vol. 82, no. 1, pp. 35–45, 1960.
2. G. Welch and G. Bishop, *An Introduction to the Kalman Filter*. Chapel Hill, NC, USA: University of North Carolina Press, 2006.
3. S. J. Julier and J. K. Uhlmann, "Unscented filtering and nonlinear estimation," *Proceedings of the IEEE*, vol. 92, no. 3, pp. 401–422, 2004.
4. D. Simon, *Optimal State Estimation: Kalman, H Infinity, and Nonlinear Approaches*. Hoboken, NJ, USA: Wiley, 2006.
5. K. P. Murphy, *Machine Learning: A Probabilistic Perspective*. Cambridge, MA, USA: MIT Press, 2012.
6. [6] C. M. Bishop, *Pattern Recognition and Machine Learning*. New York, NY, USA: Springer, 2006.
7. Gelman, J. B. Carlin, H. S. Stern, and D. B. Rubin, *Bayesian Data Analysis*, 3rd ed. Boca Raton, FL, USA: CRC Press, 2014.
8. S. S. Rao, *Engineering Optimization: Theory and Practice*, 4th ed. Hoboken, NJ, USA: Wiley, 2009.
9. K. Jennions, *Integrated Vehicle Health Management: Perspectives on an Emerging Field*. Warrendale, PA, USA: SAE International, 2011.
10. Li, Y. Liu, and Z. Tian, "Fault diagnosis of gas turbine systems using Kalman filtering methods," *Mechanical Systems and Signal Processing*, vol. 85, pp. 251–266, 2017.
11. Saxena and K. Goebel, "Turbofan engine degradation simulation data set," *NASA Ames Prognostics Data Repository*, NASA, Moffett Field, CA, USA, 2008.
12. B. Rawlings and J. G. Ekerdt, *Chemical Reactor Analysis and Design Fundamentals*. Madison, WI, USA: Nob Hill Publishing, 2012.
13. T. Kailath, A. H. Sayed, and B. Hassibi, *Linear Estimation*. Upper Saddle River, NJ, USA: Prentice Hall, 2000.
14. Y. Bar-Shalom, X. R. Li, and T. Kirubarajan, *Estimation with Applications to Tracking and Navigation*. New York, NY, USA: Wiley, 2001.
15. V. Rao and B. Kulkarni, "Gas turbine performance monitoring and diagnostics using hybrid estimation techniques," *Journal of Engineering for Gas Turbines and Power*, vol. 142, no. 6, pp. 1–10, 2020.

1. Parvin, A., and Schroeder, J. (2008). "Investigation of eccentrically loaded CFRP-confined elliptical concrete columns." J. Compos. Constr., 12(1), 93–101.
2. El-Maaddawy, T., El-Sayed, M., and Abdel-Magid, B. (2010). "The effects of cross-sectional shape and loading condition on performance of reinforced concrete members confined with carbon fiber-reinforced polymers." Mater. Des., 31(5), 2330–2341.
3. Barros JA, Ferreira DR, Fortes AS, Dias SJ. Assessing the effectiveness of embedding CFRP laminates in the near-surface for structural strengthening. Constr Build Mater 2006;20(7):478–91.
4. Barros JA, Varma RK, Sena-Cruz JM, Azevedo AF. Near-surface-mounted CFRP strips for the flexural strengthening of RC columns: Experimental and numerical research. Eng Struct 2008;30(12):3412–25.
5. Perrone, M., Barros, J. A., & Aprile, A. (2016). CFRP-based strengthening technique to increase the flexural and energy dissipation capacities of RC columns. J. Compos. Constr. 2009;13(5):372–83.
6. Bournas DA, Triantafillou TC. Flexural strengthening of RC columns with NSM FRP or stainless steel. ACI Struct J 2009;106(4):495–505.
7. Ding L, Wu G, Yang S, Wu Z. Performance advancement of RC columns by applying basalt FRP composites with NSM and confinement system. J Earthq Tsunami 2013; 7(2):1–20.
8. Hasan QF, Tekeli H, Demir F. NSM Rebar and CFRP laminate strengthening for RC columns subjected to cyclic loading. Constr Build Mater 2016;119:21–30.
9. Fahmy MF, Wu Z. An exploratory study of the seismic response of deficient lap-splice columns retrofitted with near–surface–mounted basalt FRP bars. J. Struct. Eng. 2016; 142(6): 1–16.
10. Seifi A, Hosseini A, Marefat MS, Khanmohammadi M. Seismic retrofitting of old-type RC columns with different lap splices by NSM GFRP and steel bars. Structural Design Tall Spec Build 2018; 27(2): 1–21.
11. Sarafraz ME, Danesh F. New technique for flexural strengthening of RC columns with NSM FRP bars. Mag Concr Res 2012; 64(2): 151–61.
12. Xing G, Ozbulut OE, Al-Dhabyani MA, Chang Z, Daghash SM. Enhancing the Flexural Capacity of RC Columns through Near-Surface-Mounted SMA and CFRP Bars. J Compos Mater 2020;54(29):4661–76.
13. (2011) El-Maaddawy, Tamer, and Amr S. El-Dieb. "Near-surface-mounted composite system for repair and strengthening of reinforced concrete columns subjected to axial load and biaxial bending." *Journal of composites for construction* 15.4 (2011): 602-614.
14. (2021) Khorramian, Koosha, and Pedram Sadeghian. "Hybrid system of longitudinal CFRP laminates and GFRP wraps for strengthening of existing circular concrete columns." *Engineering Structures* 235 (2021): 112028
15. (2019) Khorramian, Koosha, and Pedram Sadeghian. "Performance of high-modulus near-surface-mounted FRP laminates for strengthening of concrete columns." *Composites Part B: Engineering* 164 (2019): 90-102.
16. (2017) Khorramian, Koosha, and Pedram Sadeghian. "Strengthening short concrete columns using longitudinally bonded CFRP laminates." *The 13th International Symposium on Fiber-Reinforced Polymer Reinforcement for Concrete Structures (FRPRCS-13), Anaheim, CA, USA*. 2017.
17. (2017) Khorramian, Koosha, and Pedram Sadeghian. "Strengthening concrete columns using NSM CFRP laminates." 6th Asia-Pacific Conference on FRP in Structures, 2017.

18. (2018) Khorramian, Koosha, and Pedram Sadeghian. "Rehabilitation of Bridge Columns Using Hybrid Strengthening Method of Longitudinal CFRP and Transverse GFRP Wraps." *10th International Conference on Short- and Medium-Span Bridges*. 2018.

19. (2020) Khorramian, Koosha. *Short and slender concrete columns internally or externally reinforced with longitudinal fiber-reinforced polymer composites*. Diss. Dalhousie University, 2020.

20. Xing, Guohua, et al. "Enhancing flexural capacity of RC columns through near-surface mounted SMA and CFRP bars." *Journal of Composite Materials* 54.29 (2020): 4661-4676.

21. Wang, Haonan, et al. "Seismic behavior of RC columns strengthened with near-surface-mounted aluminum alloy bars and CFRP wraps." *Engineering Structures* 268 (2022): 114742.

22. Abokwiek, Raed, et al. "RC columns strengthened with NSM-CFRP strips and CFRP wraps under axial and uniaxial bending: experimental investigation and capacity models." *Journal of Composites for Construction* 25.2 (2021): 04021009.

23. Gajdosova, Katarina, and Juraj Bilcik. "Full-scale testing of CFRP-strengthened slender reinforced concrete columns." *Journal of Composites for Construction, 17 (2), 2013, pp.* 239-248.

24. Khorramian, Koosha, and Pedram Sadeghian. "Slender RC columns strengthened with a novel hybrid strengthening system of external longitudinal and transverse FRPs." *Journal of Structural Engineering* 147.10 (2021): 04021154.

25. Khorramian, Koosha, and Pedram Sadeghian. "Strengthening slender circular concrete columns with a novel hybrid FRP system." *CSCE Annual Conference 2018, Fredericton, NB, Canada*. 2018.

26. Radhi, Mushtaq S., Maan S. Hassan, and Iqbal N. Gorgis. "Carbon fibre-reinforced polymer confinement of corroded circular concrete columns." *Journal of Building Engineering* 43 (2021): 102611.

27. Chellapandian, M., S. Suriya Prakash, and Akanshu Sharma. "Experimental and finite element studies on the flexural behavior of reinforced concrete elements strengthened with hybrid FRP technique." *Composite Structures* 208 (2019): 466-478.

28. Chinthapalli, Hemanth Kumar, et al. "Effectiveness of hybrid fibre-reinforced polymer retrofitting on behaviour of fire-damaged RC columns under axial compression." *Engineering Structures* 211 (2020): 110458.

29. Van Cao, Vui, et al. "Monotonic/cyclic behavior of postfire RC beam-column joints without/with CFRP retrofitting: Experiments." *Journal of Building Engineering* (2025): 113371.

30. Cetin, Kabil, Taha Yasin Altiok, and Ali Demir. "Experimental investigation of EBROG and bore-epoxy anchorage methods used for interior RC beam-column joints strengthened with CFRP sheets." *Structures*. Vol. 66. Elsevier, 2024.

31. Wang, Guo-Lin, Jian-Guo Dai, and Yu-Lei Bai. "Seismic retrofit of exterior RC beam-column joints with bonded CFRP reinforcement: An experimental study." *Composite Structures* 224 (2019): 111018.

32. Saqan, Elias I., Hayder A. Rasheed, and Tarek Alkhrdaji. "Evaluation of the seismic performance of reinforced concrete frames strengthened with CFRP fabric and NSM bars." *Composite Structures* 184 (2018): 839-847.